

drive the oscillation, and this threshold density increases with increasing temperature. At fixed beam density the instability will become convective when the plasma is made effectively warmer, since the given density will become smaller than the threshold value. The experimental results are thus due to the changes in threshold beam density in response to changes in the thermal parameters. In Figs. 1 and 2  $v_t/V$  is changed, and in Fig. 3 the threshold increases as  $k_{\perp}v_t/\omega_c$  increases and also as  $\omega$  approaches  $n\omega_c$ , where  $\omega - n\omega_c \approx 0$ .

In this experiment the plasma can be made effectively warm enough so that we have convective instability at the maximum attainable beam density ( $\omega_B^2/\omega_P^2 \approx 10^{-2}$ ). In terms of thermal parameters this occurs when  $k_{\perp}v_t/\omega_c > 0.1$  and  $V/v_t < 10$ .

From this work we conclude that plasma thermal effects must be considered in the analysis of  $H$ -wave experiments, since either convective or absolute instability may be present. We have examined experiments on the  $H$  wave by other workers, and conclude that the observed waves were absolute instabilities<sup>3,9,10</sup> except for the work of Mizuno and Tanaka.<sup>4</sup> There the cold-

plasma dispersion relation was erroneously used to describe a convective instability.

\*Work supported by the National Science Foundation and the U. S. Air Force Office of Scientific Research.

<sup>1</sup>M. Seidl, Phys. Fluids **13**, 966 (1970).

<sup>2</sup>R. J. Briggs, *Electron-Stream Interactions with Plasmas* (Massachusetts Institute of Technology Press, Cambridge, Mass., 1964), p. 165.

<sup>3</sup>J. H. A. van Wakeren and H. J. Hopman, Phys. Rev. Lett. **28**, 285 (1972).

<sup>4</sup>K. Mizuno and S. Tanaka, Phys. Rev. Lett. **29**, 45 (1972).

<sup>5</sup>Briggs, Ref. 2, p. 101.

<sup>6</sup>W. Carr, D. Boyd, H. Liu, G. Schmidt, and M. Seidl, Phys. Rev. Lett. **28**, 662 (1972).

<sup>7</sup>Briggs, Ref. 2, p. 30.

<sup>8</sup> $\text{Im}(\omega)$  and  $\text{Im}(k)$  have signs opposite to those of Ref. 7, since there the wave is of the form  $\exp[i(\omega t - k_z z)]$ .

<sup>9</sup>I. F. Kharchenko *et al.*, Zh. Tekh. Fiz. **34**, 1031 (1964) [Sov. Phys. Tech. Phys. **9**, 798 (1964)]; M. Seidl and P. Sunka, Nucl. Fusion **7**, 237 (1967); T. Idehara, J. Phys. Soc. Jap. **23**, 660 (1967).

<sup>10</sup>V. Piffel *et al.*, in *Proceedings of the Fourth International Conference on Plasma Physics and Controlled Nuclear Fusion Research, Madison, Wisconsin, 1971* (International Atomic Energy Agency, Vienna, 1972), Vol. II, p. 733.

## Evolution of Bernstein-Greene-Kruskal-like Ion Modes with Trapped Electrons

A. Y. Wong, B. H. Quon, and B. H. Ripin

*Department of Physics, University of California, Los Angeles, California 90024*

(Received 20 April 1973)

The growth of an ion acoustic instability caused by a slow electron drift is studied experimentally. A small-amplitude test wave in this unstable system develops into a large-amplitude steady state which is found to be a Bernstein-Greene-Kruskal-like ion mode with trapped electrons.

We wish to report experimental observations of the spatial growth of ion acoustic waves in the presence of a slow electron drift.<sup>1</sup> The final state of the wave, which does not decay spatially, together with the measured distribution function, appear to be consistent with Bernstein-Greene-Kruskal (BGK) modes<sup>2</sup> with trapped electrons. Although theoretically predicted,<sup>2</sup> such modes have not been observed experimentally. The temporal or spatial evolution of such BGK modes have not been studied extensively either, presumably because of a lack of experimental evidence.

In our experiments we have chosen experimen-

tal parameters (density, temperature, and neutral pressures) such that electrons can execute many bounces in the ion acoustic wave potential well within a collisional time. For either ions trapped in ion waves<sup>3</sup> or electrons trapped in electron waves,<sup>4,5</sup> the bounce time of the trapped particles is usually slower than the wave period and it is difficult to observe experimentally steady-state or quasi-steady-state behavior. However, the large electron-to-ion temperature ratio ( $T_e/T_i \approx 15$ ) and the high phase velocity of the ion acoustic wave favor the trapping of electrons rather than ions in our experiment. In order to facilitate the identification of trapped

electrons we have chosen to look at the change of the positive slope in the initial electron distribution function as the growth of ion acoustic waves takes place. The slow electron drift velocity also enables the ion acoustic wave to grow from an excitation sufficiently small so that other complicating effects are avoided. This procedure is to be contrasted with the usual approach of exciting a large-amplitude wave by a large source voltage and the subsequent examination of trapping near the source. This latter method can produce pseudowaves and ballistic effects which may complicate the subsequent interpretations.

The experimental arrangement is the University of California, Los Angeles, double plasma device,<sup>6</sup> modified to reduce axial density gradients, in which an electron drift is generated by biasing one plasma chamber positive with respect to another. This technique produces a slow electron drift [ $u \approx 0.25a_e$ , where  $a_e$  is the electron thermal speed, i.e.,  $a_e = (2\kappa T_e/m)^{1/2}$ ], throughout a large diameter (30 cm) in a plasma of equally large diameter. The experimental results can therefore be directly compared with theories for homogeneous plasmas. Our operating conditions are  $10^8 < n_0 < 10^9 \text{ cm}^{-3}$ ,  $\kappa T_e \approx 2 \text{ eV}$ ,  $T_e/T_i \approx 15$ . At the operating pressure of 0.2 to  $0.4 \mu\text{m}$  in argon the mean free paths for electron-neutral collisions and electron-ion collisions are greater than the plasma dimensions. There is, however, a small density gradient  $n_0^{-1} \partial n_0 / \partial x \approx 0.01 \text{ cm}^{-1}$  in the axial direction, the same direction as the drift velocity. Movable axial planar probes are used to monitor the growth of the ion acoustic waves which start either from thermal noise level or from a small test signal applied to one of the two separation grids of the double plasma device. Electron distribution functions are simultaneously measured by differentiating the probe current characteristics with respect to the probe voltage.

When the bias between the two chambers is adjusted to give an electron drift such that the positive slope of the electron distribution function coincides with the phase velocity of an ion acoustic wave, a noise spectrum which peaks at  $\omega/\omega_{pi} \approx 0.5$  with a width  $\Delta\omega/\omega_{pi} \approx 0.15$  between 3-dB points is observed ( $\omega_{pi}$  is the ion plasma frequency). This unstable spectrum was identified as that of ion acoustic waves through the measurements of the wave dispersion (Fig. 1) for small wave amplitudes  $n_1/n_0 \approx 0.01$ . Two methods of measurements are used. The first method in-

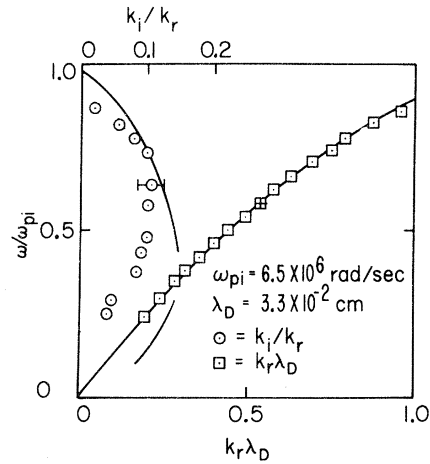


FIG. 1. Linear dispersion of unstable ion acoustic waves in the presence of a slow electron drift. Solid lines are theoretical dispersion relations including ion-neutral collisions. Plasma conditions:  $\kappa T_e \approx 2 \text{ eV}$ ,  $T_e/T_i = 15$ ,  $n_0 \approx 10^8 \text{ cm}^{-3}$ , and  $\nu_{in} \approx 6 \times 10^4 \text{ sec}^{-1}$ .

volves spatial correlation measurements at a particular frequency, using two sharply tuned filters and two probes whose separation can be continuously varied. The second method requires the excitation of a small test wave (excitation voltage  $\sim 5 \text{ mV}$ , which is about the same level as the background noise) whose spatial growth and phase change can be compared with a well-defined reference. The linear growth rate  $k_i/k_r$  is compared with the numerical solutions of the linear dispersion relation of ion acoustic waves.<sup>7</sup> The dispersion relation in the presence of an electron drift  $u$  including collisionals with neutrals<sup>8</sup> is

$$\frac{2k^2}{k_e^2} = Z' \left( \frac{\omega - \vec{k} \cdot \vec{u} + i\nu_{en}}{\kappa a_e} \right) + \frac{T_e}{T_i} Z' \left( \frac{\omega + i\nu_{in}}{\kappa a_i} \right),$$

where  $Z'$  is the derivative of the plasma dispersion function,<sup>9</sup>  $k_e = \sqrt{2}\omega_{pe}/a_e$  is the electron Debye wave number,  $a_i$  is the ion thermal speed, and  $\nu_{en}$  and  $\nu_{in}$  are the electron-neutral collision frequency and ion-neutral collision frequency, respectively. At the operating pressure ( $\nu_{en} \approx 2 \times 10^5 \text{ sec}^{-1}$ ,  $\nu_{in} \approx 6 \times 10^4 \text{ sec}^{-1}$ ) the ion-neutral collisions account for the dominant reduction of the collisionless growth rate. The real part of the wave dispersion is seen to follow closely the ion acoustic branch in Fig. 1. Note from Fig. 1 that the electron drift and the small collisional effect favors the growth over only a limited frequency

spectrum, with the most unstable wave propagating along the electron drift velocity. In the case of a test wave the planar excitation over a large cross section further favors the one-dimensional propagation along the drift direction. The experimentally observed growth rates are in good qualitative agreement with the theory (Fig. 1). The apparent reduction of the measured growth rates with respect to the theory might be due to trapping effects or wave-particle collision processes in the presence of the unstable waves. Both these effects become important even at the amplitude  $n_1/n_0 \approx 0.01$  where the measurements take place, e.g., at this amplitude the bounce frequency  $\omega_b = [(M/m)e\phi_0/\kappa T_e]^{1/2}\omega$  is already comparable to the effective electron-electron collision frequency  $\nu_{eff} = \nu_{ee}(\kappa T_e/e\phi_0) \approx 2 \times 10^6 \text{ sec}^{-1}$ .<sup>10</sup>

The most interesting part of the experiment is the growth of an ion acoustic wave (over 30 dB) to a steady-state large-amplitude ( $n_1/n_0 \approx e\phi_0/\kappa T_e \approx 10\%$ ) sinusoidal wave which is constant over 10 wavelengths, limited essentially by the constancy of the spatial zeroth-order conditions. A sampled wave form, obtained using a boxcar integrator (PAR-160), is shown in Fig. 2. This BGK-like ion acoustic mode is observed under the following experimental conditions: First, a test-wave signal is excited with frequency near the peak of the growth spectrum, i.e., the most unstable wave frequency. The excitation voltage is sufficiently small (25–50 mV) such that pseudowaves and ballistic waves are not produced by the excitation grid. However, the test-wave signal is larger than the background noise near the grid so that the test-wave amplitude exceeds that of the spontaneous noise within a short distance (by at least 10 dB) as it propagates along the direction of the electron drift velocity. Higher harmonics, subharmonics, and shocks are not produced because of the limited frequency spectrum of the unstable waves; for example, the second-harmonic content is at least 20 to 30 dB below the fundamental.

The correlation between the spatial development of the test ion acoustic wave and the spatial evolution of the electron distribution  $f(E)$  is demonstrated in Fig. 2. To distinguish the electron trapping effect from the time-averaged spatial development of the distribution,<sup>11</sup> a sampling technique is adopted in this experiment. The distribution function at each spatial location is measured using a box-car integrator, which synchronously samples the probe current signal at

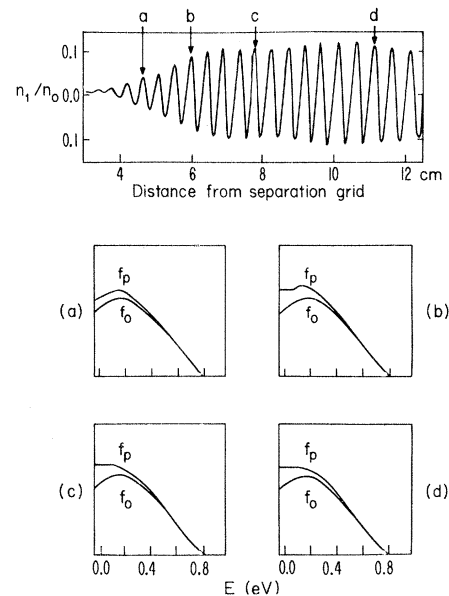


FIG. 2. Correlation between the spatial growth of an ion acoustic wave and the evolution of the electron distribution. The wave frequency  $f = 480 \text{ kHz}$ , excitation voltage = 25 mV, maximum wave amplitude  $n_1/n_0 = e\phi_0/\kappa T_e = 0.1$ .  $E$  is the electron energy with respect to the plasma potential,  $f_p$  is the distribution function sampled at the positive maximum of the wave potential, and  $f_0$  is the zeroth-order distribution function sampled without a test wave. (a)–(d) The distribution function is sampled at spatial points  $a$ – $d$  and the zero level has been suppressed to magnify the trapping region.

a specific phase of the ion acoustic wave, such that the detailed information is not averaged out by potential fluctuations. The sampled probe current signal is then differentiated by using a lock-in technique<sup>12</sup> to obtain the electron distribution function. A tone-burst test wave is often used in place of a cw test wave to avoid any possibility of interference due to a direct pickup signal. As the amplitude of the ion acoustic wave grows toward its steady-state value the portion of the zeroth-order electron distribution function with positive slope, where the phase velocity of the ion acoustic wave lies, becomes progressively flatter. It is important to note that this characteristic only occurs where the ion acoustic wave potential is positive and where electrons are expected to be trapped. Quasilinear theory would have predicted the same characteristics everywhere. The energy of electrons moving at the phase velocity of the ion acoustic wave is designated as the zero reference point in our distribution function diagrams of  $f(E)$  versus  $E$ . This reference point is different from the plasma potential by only a small amount  $\Delta\phi \approx (m/M)\kappa T_e$ .

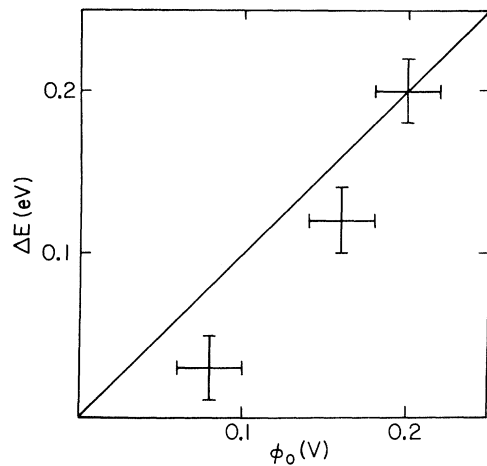


FIG. 3. Observable trapping region  $\Delta E$ , which is the extent of the flat region near the top of the electron distribution, versus the maximum wave amplitude  $\phi_0$ .

The plasma potential is determined by an emissive probe method and corresponds to the probe bias voltage at which a large emission of electrons by a heated probe is observed.<sup>13</sup>

The large-amplitude ion acoustic wave is expected to create the observed flattened electron distribution function in the trapping region from the initial distribution.<sup>14</sup> To check whether the experimentally observed state is consistent with the BGK theory we performed the self-consistent calculations as outlined by BGK.<sup>2</sup> The results indicate that the observed trapped-electron distribution which is independent of energy in the trapping region,  $E < e\phi_0$ , is self-consistent with the observed ion wave and does constitute an acceptable BGK solution. Furthermore, for  $e\phi_0/\kappa T_e \approx 0.1$ , the theoretically required trapped-electron density,  $n^t$ , agrees with the measured value  $n^t \approx 0.2n_0$  within the experimental accuracy. Details of this calculation will be published elsewhere.

The extent of the flattened portion of  $f(E)$  is directly proportional to the maximum potential  $\phi_0$  of the ion acoustic wave (as shown in Fig. 3). This is expected from the criterion of trapping, i.e., particles whose energy  $E < e\phi_0$  may become trapped in the ion waves. The difference between the areas under the two distribution functions

sampled at the peaks and troughs of the ion wave yields a measure of the density fluctuation.

In summary we have measured for the first time (1) the linear spatial growth rate of ion acoustic waves in the presence of a slow electron drift, (2) a constant saturated state of the ion acoustic wave which resembles a BGK mode, and (3) the development of a trapped-electron distribution function.

We wish to acknowledge useful discussions with Dr. N. Albright, Dr. G. Schmidt, and Dr. S. Hamberger.

\*This work was supported by the National Science Foundation under Grant No. NSF GP-28509X1.

<sup>1</sup>E. A. Jackson, *Phys. Fluids* **3**, 786 (1960); B. D. Fried and R. W. Gould, *Phys. Fluids* **4**, 139 (1961); Y. Amagishi, *Phys. Rev. Lett.* **29**, 405 (1972), and *J. Phys. Soc. Jap.* **29**, 1592 (1970); M. Fujiwara, M. Raether, and M. Yamada, *J. Phys. Soc. Jap.* **27**, 758 (1969); B. H. Quon, B. H. Ripin, and A. Y. Wong, *Bull. Amer. Phys. Soc.* **17**, 1041 (1972).

<sup>2</sup>I. B. Bernstein, M. Greene, and M. D. Kruskal, *Phys. Rev.* **108**, 546 (1957).

<sup>3</sup>H. Ikezi, Y. Kiwamoto, K. Nishikawa, and K. Mima, *Phys. Fluids* **15**, 1605 (1972).

<sup>4</sup>K. W. Gentle and J. Lohr, *Phys. Rev. Lett.* **30**, 75 (1973).

<sup>5</sup>R. N. Franklin, S. M. Hamberger, and G. J. Smith, *Phys. Rev. Lett.* **29**, 914 (1972).

<sup>6</sup>R. J. Taylor, K. R. MacKenzie, and H. Ikezi, *Rev. Sci. Instrum.* **45**, 1675 (1972).

<sup>7</sup>T. E. Stringer, *Plasma Phys.* **6**, 267 (1964); N. Albright, private communication.

<sup>8</sup>P. L. Bhatnagar, E. P. Gross, and M. Krook, *Phys. Rev.* **94**, 511 (1954).

<sup>9</sup>B. D. Fried and S. Conte, *The Plasma Dispersion Function* (Academic, New York, 1961).

<sup>10</sup>K. Nishikawa and C. S. Wu, *Phys. Rev. Lett.* **23**, 1020 (1969).

<sup>11</sup>J. A. Wesson, A. Sykes, and H. R. Lewis, *Plasma Phys.* **15**, 49 (1973).

<sup>12</sup>P. J. Barrett, D. Gresillon, and A. Y. Wong, in *Proceedings of the Third International Conference on Quiet Plasma, Elsinore, Denmark, 1971* (Jul. Gjellerups Forlag, Copenhagen, Denmark, 1971).

<sup>13</sup>R. F. Kemp and J. M. Sellen, *Rev. Sci. Instrum.* **37**, 455 (1966).

<sup>14</sup>R. Z. Sagdeev and A. A. Galeev, in *Nonlinear Plasma Theory*, edited by T. M. O'Neil and D. L. Book (Benjamin, New York, 1969).